Comparison between Mode I and Mode III crack propagation under pure shear and RCF conditions

S. Beretta, S. Foletti, M.G. Tarantino
Politecnico di Milano, Department of Mechanical Engineering, Milano (Italy)
stefano.beretta@polimi.it

J. Lai
SKF Engineering and Research centre, Nieuwegein, The Netherlands

ABSTRACT. The competition between mode I and mode III failure modes on the experimentally results obtained by the authors during an extensive experimental campaign under pure shear and RCF loading conditions on both a bearing and a gear steel have been analysed. The analysis of the fracture surfaces has shown that the failure of the torsional samples is a tensile fracture, while the OOP samples failed by shear fracture. In order to understand the competition between the two failure modes (Mode I vs. Mode III) the loading patterns have been analysed in terms of mode I and mode III branch stress intensity factors and the experimental fracture behaviour has been confirmed by theoretical predictions when a partial slip model, previously employed by the authors, is used.

KEYWORDS. Mode I; Mode III; Crack growth; Shear propagation; RCF; Friction.

INTRODUCTION

Mode III fatigue crack behaviour have been investigated by some researchers in order to better understand the complex mechanism of crack path under this loading condition [1]. Both turbine-generator shafts under transient torsional loading and components under rolling contact fatigue, (such as bearings, gears, rails and etc), exhibit mode III crack propagation. Since the fatigue failures of the mechanical components previously mentioned inevitably result in costly engineering damage/loss and down-time, it is of some importance to deep inside the mode III fatigue crack behaviour.

Experimental investigations have shown that the mode III crack growth fracture features depends on the local mode mixity at the crack tip which may be very different from that evaluated on the basis of the external loadings only.

The fracture surfaces of a circumferentially notched shaft [2] tested under pure shear were found to be very tortuous, resulting in a crack front rotation and segmentation often called factory roof crack surface. Tschegg and Nayeb-Hashemi et al [3-4] experiments revealed that a superimposed static axial load on the fatigue in torsion can promote stable mode III crack growth, since it reduces the sliding mode crack growth effect. According to Tschegg there is a critical applied stress intensity factor value under which mode III crack propagation is no more stable, resulting in a mode I branching and this nominal value of the applied ΔK_{III} can be interpreted as a mode III fatigue threshold since the fracture mode changes from a macroscopically flat (mode III) to a factory roof (mode I) type.

The aim of the present study is to analyse the competition between mode I and mode III failure modes which have been experimentally observed by the authors during an extensive experimental campaign under pure shear and RCF loading conditions on both a gear [5-6] and a bearing steel material [7].

EXPERIMENTAL DETAILS

Materials

The materials analyzed is a bearing steel. The basic properties and the fatigue behaviour of the material were first determined. Tab. 1 summarizes the results of monotonic and cyclic tests. The material showed a strain hardening behaviour when subjected to cyclic loading.

Material	UTS [MPa]	σ_y [MPa]	$\sigma_{y,cyclic}$ 0.2% [MPa]
Bearing steel	2364	1982	2072

Table 1: Materials mechanical properties.

Specimens

All fatigue tests were carried out on pre-cracked micro-notched hourglass specimens. Three defect sizes, expressed in terms of Murakami's √area parameter, equal to 630 μm, 315 μm and 220 μm have been considered. The bearing steel specimens geometry and micro-notches adopted are presented in Fig. 1. The specimens geometry can be found in [7].

Before starting the tests, all specimens were electro polished to avoid the effect of the surface residual stresses. Then, artificial micro notches were introduced by means of electro-discharging machining (EDM). In order to promote co-planar crack propagation, a preliminary Mode I fatigue test pre-cracking procedure was adopted. All specimens were subject to push-pull axial fatigue for 1.0×10^7 cycles at R=-2 at a stress level close to $\Delta K_{th,I}$ till $N_f = 10^7$.
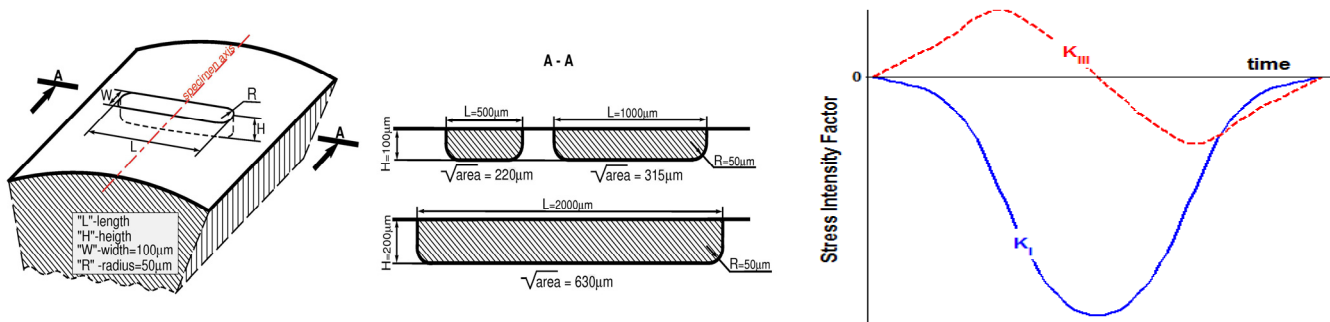
Figure 1: Fatigue tests samples: a) micro-notches used; b) load pattern schemes adopted for OOP multiaxial fatigue tests.

Pre-cracking procedure induced small non-propagating cracks at the bottom of the notch with a depth of approximately 20 μm. All specimens were observed under SEM for verifying the success of pre-cracking procedure (if not successful the Mode I loading was repeated).

Fatigue tests

After the pre-cracking procedure, the specimens were subjected to torsional or multiaxial fatigue tests. The main idea of the experimental onset is to run fatigue tests decreasing the load from one specimen to another till no fatigue crack growth will occur. During the fatigue tests an optical microscope Leica system permitted to control surface mixed-mode crack advance continuously during the test.

Torsional fatigue tests were carried out at stress ratio of R= -1 using a RUMUL CRACKTRONIC resonance machine (capacity ± 90Nm) operating at an average frequency of 60 Hz.

Multiaxial fatigue tests were conducted in force/torque control by means of a MTS 809 Axial Torsional System. Fatigue tests were carried out adopting torsion/push-pull sequence under load control (frequency=2 Hz) simulating conditions of subsurface RCF in bearings. The load patterns were supplied by SKF and loaded point by point into the test rig controlling software; the load pattern scheme used for multiaxial fatigue tests is reported in Fig.1b.

Multiaxial fatigue test were interrupted on the basis of the maximum surface crack length measurements $a_s<1$ mm otherwise in the according to the number of fatigue cycles ($N_f = 2 \cdot 10^6$) as if near threshold crack propagation was of interest.

FATIGUE TEST RESULTS

The experimental fracture surface morphologies demonstrate that there is a failure transition from tensile (Mode I) to shear (Mode III) type.

The analysis of the fracture surfaces of the torsional samples shows that failures always occurred in Mode I on tilted fracture planes at 45°, see Fig. 2, which had been nucleated along thin shear cracks at the bottom of the micronotches as well as the evidence of two main types of coplanar growth regimes: the first, named 'discontinuous' growth, observed at a ΔK_{III} level close to $\Delta K_{th,I}$, and characterised by the formation of so called semi-elliptical Mode III 'pockets'; the second, named 'continuous' coplanar growth and characterised by stable Mode III coplanar growth. The Mode III threshold $\Delta K_{th,III}$, corresponding to a 'discontinuous' co-planar crack, is very close to $\Delta K_{th,I}$.

a)

b)
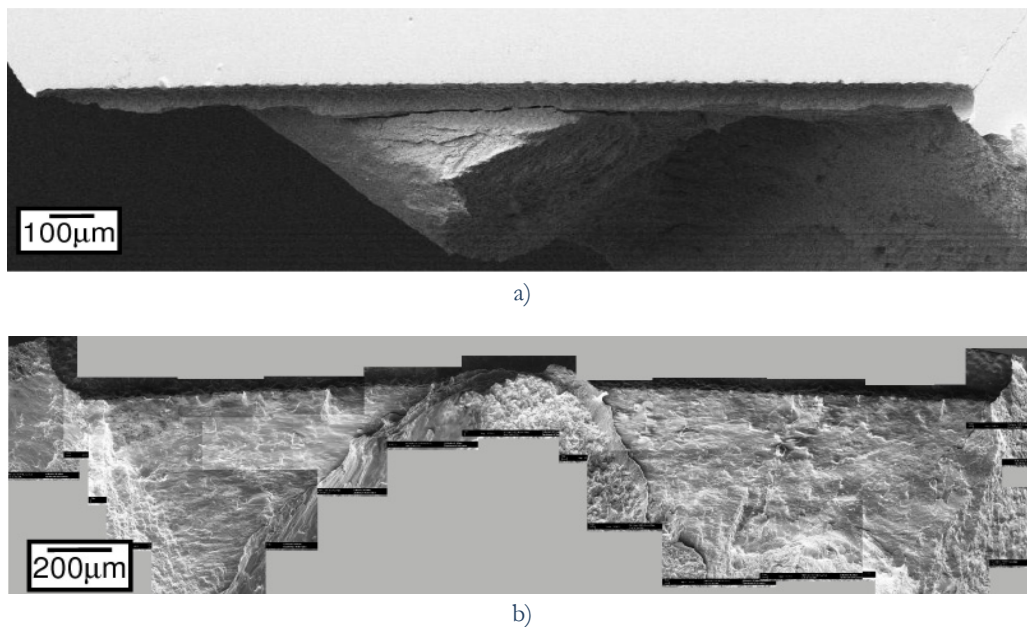
Figure 2: Continuous coplanar crack SEM photos of a torsional sample after static rupture ($\sqrt{area} = 630\mu m$, $\Delta K_{III}/\Delta K_{th,I} = 1.75$ broken at $N_f = 3 \cdot 10^3$): top view; b) 90° tilted view.

The analysis of the fracture surfaces of the multiaxial samples clearly shows that out-of-phase load pattern (axial force always in compression and shifted 90 degrees in respect to alternating torsion) enhances crack growth rate and leads to a severe reduction of the minimum ΔK_{III} at which co-planar crack growth could occur (continuous Mode III propagation was obtained at ΔK_{III} levels much lower than Mode I threshold) and inhibits the development of Mode I kinked cracks (Fig. 3).

The other distinctive feature of the 'OOP load pattern growth' is the fact that crack advance is characterized (both for the present bearing steel and the previous gear steel [5,7]) by a residual crack opening caused by plastic deformation and wear (recognizable on account of the large amount of debris). Sectioning of a specimen tested at $\Delta K_{III}/\Delta K_{th,I} = 0.8$ (test interrupted at $N = 2 \cdot 10^5$ cycles) showed a value of the crack opening almost constant within the whole coplanar crack depth (Fig. 4b) as well as the typical appearance of a crack under RCF loading conditions (Fig. 4c); several sub-surface multiple sites of crack branching were also observed at the main co-planar crack propagation site.

OOP test results together with pure torsional tests are shown in the Fig. 5a. Due to confidentiality issues, experimental results are presented in normalised form, with ΔK_{III} normalised respect to the $\Delta K_{Ith,LC}$ for long cracks.

COMPARISON BETWEEN MODE I AND MODE III

In order to understand the competition between the two failure modes (Mode I vs. Mode III) we have examined the loading patterns in terms of mode I and mode III branch stress intensity factors. The basis for the calculation is the near-field solution for stress distribution at the crack front [8].

Resolving the stress state onto a tilted plane, identified by an angle ψ (see Fig. 5b), the Mode I and Mode III branch crack stress intensity factors were obtained by multiplying the tensile stress $\sigma_{\varphi'}$ and the shear stress $\tau_{\varphi'z'}$ near the tip of a branch crack by $(2\pi r)^{0.5}$, Eq.(1):

$$\begin{cases} k_I\left(\varphi,\psi,t\right) = K_I\left(t\right)\left[\cos^3\left(\frac{\varphi}{2}\right)\cos^2\left(\psi\right) + 2\nu\cos\left(\frac{\varphi}{2}\right)\sin^2\left(\psi\right)\right] - K_{III}\left(t\right)\cos\left(\frac{\varphi}{2}\right)\sin\left(2\psi\right) \\ k_{III}\left(\varphi,\psi,t\right) = K_I\left(t\right)\left[\frac{1}{2}\cos^3\left(\frac{\varphi}{2}\right)\sin\left(2\psi\right) - \nu\cos\left(\frac{\varphi}{2}\right)\sin\left(2\psi\right)\right] + K_{III}\left(t\right)\cos\left(\frac{\varphi}{2}\right)\cos\left(2\psi\right) \end{cases} \tag{1}$$

where K_I and K_{III} are the nominal stress intensity factors calculated at the bottom of the micro-notch.

At each step of the loading cycle the maximum value of both Mode I and Mode III branch crack stress intensity factor were found by maximizing the analytical expression of $k_I(\varphi,\psi)$ and $k_{III}(\varphi,\psi)$ in respect to the angles φ and ψ, i.e. :

$$\begin{aligned} k_{I,max}\left(t\right) &= \max_{(\varphi,\psi)}\left(k_I\left(\varphi,\psi,t\right)\right) \\ k_{III,max}\left(t\right) &= \max_{(\varphi,\psi)}\left(k_{III}\left(\varphi,\psi,t\right)\right) \end{aligned} \tag{2}$$

We have examined the samples tested at values of $\Delta K_{III}/\Delta K_{th,I}$ equal to and lower than the threshold (characterized by a 'discontinuous' or 'absent' mode III propagation respectively). Results, normalized with respect to the maximum value of the Mode I threshold $K_{th,I,MAX}$ for small cracks, are shown in Fig. 6a for the biggest size of the micro-notch ($\sqrt{area}$ 630 μm). Similar results could be obtained for micro-notch size $\sqrt{area} = 220\mu$m.
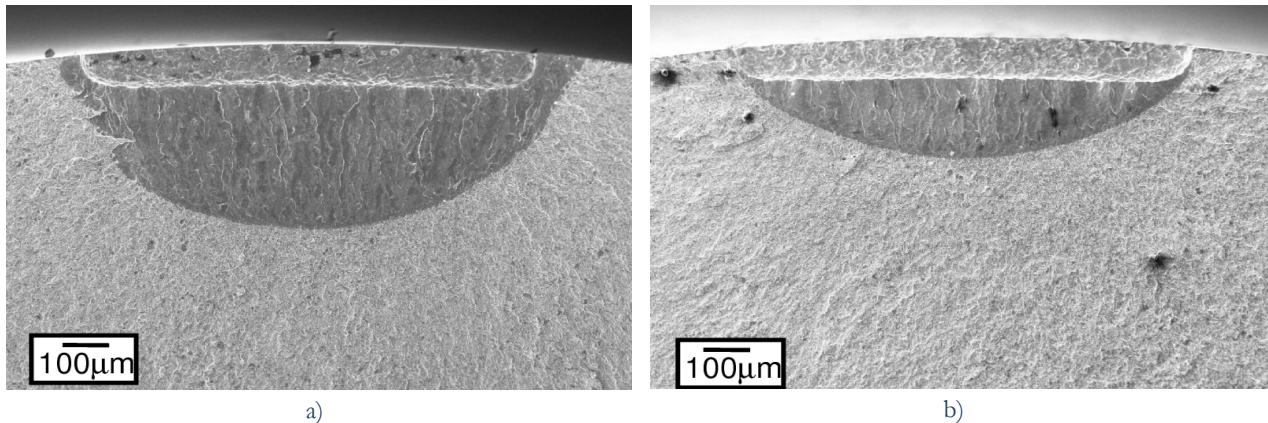
Figure 3: Multiaxial Fatigue Test, Mode III fracture surfaces $\sqrt{area} = 315\mu$m: a) specimen tested at $\Delta K_{III}/\Delta K_{th,I} = 0.87$ for N $= 10^4$ cycles; b) specimen tested at $\Delta K_{III}/\Delta K_{th,I} = 0.7$ for N $= 1.2\cdot10^5$ cycles

Fig. 6a explains why, for a small co-planar crack ahead of the micro-notch, Mode I cannot compete with the shear propagation in OOP load pattern experiments since k_I is always negative, contrarily to what happens in torsional tests where on tilted planes at $\theta=45°$ $k_I=K_{III}$ [5]. However, the OOP load path is always below the nominal mode III threshold $K_{th,III,MAX}$ thereby indicating that the crack should not start to propagate under mode III: in fact during the loading cycle, the local mode III SIF, never exceeds the maximum value of the Mode III threshold $K_{th,III,MAX}$. On the contrary, the SEM photos of the fractographic surfaces at the threshold condition ('discontinuous growth') (Fig.s 6b), show evidence of shear propagation.
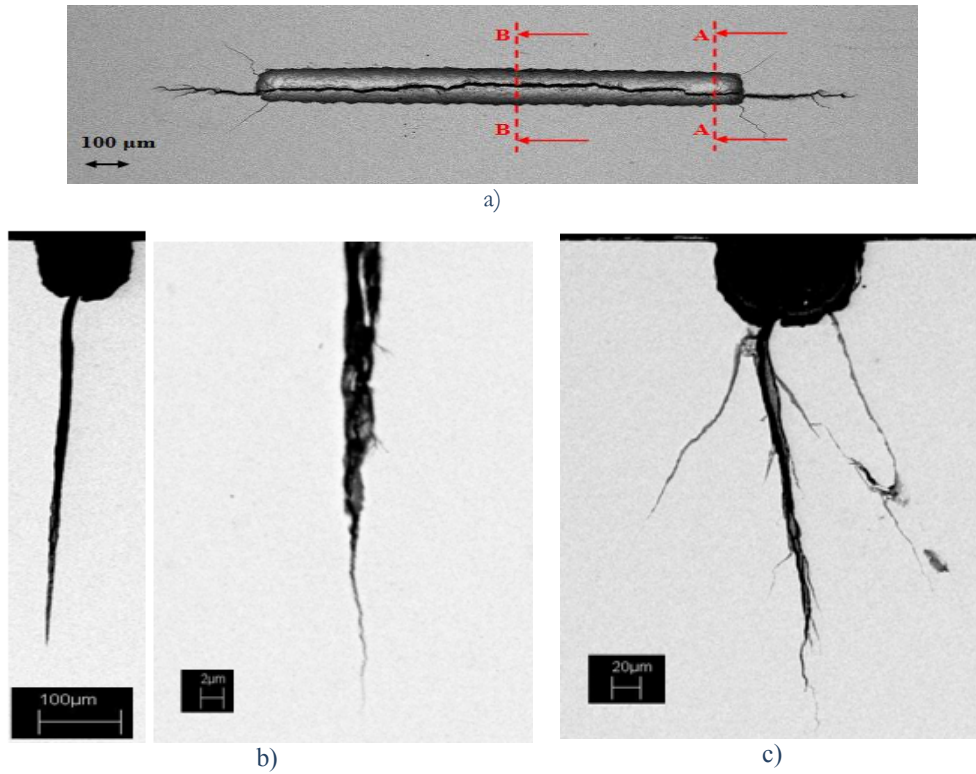
Figure 4: Multiaxial fatigue specimen tested at $\Delta K_{III}=0.8\Delta K_{th,I}$, test interrupted at N = $2 \cdot 10^5$ cycles, $\sqrt{area}$ = 315μm: a) specimen surface; b) central area section (section B-B) and a magnification; c) typical appearance of a RCF crack (section A-A).
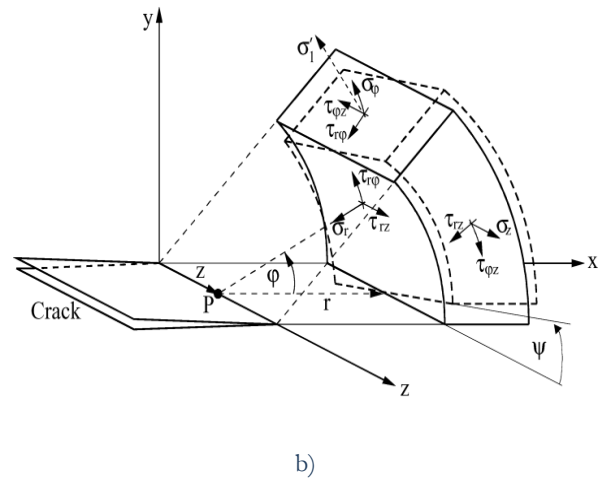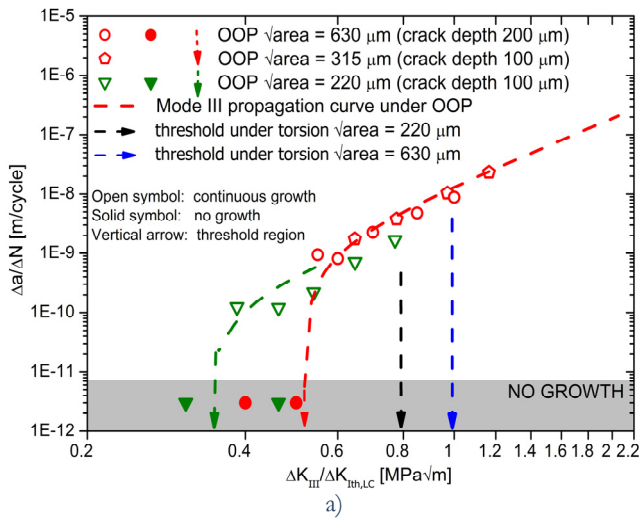
Figure 5: a) Coplanar Mode III average growth rates present OOP multiaxial fatigue test together with pure torsional tests; b) cylindrical coordinate system

Competitions between the failure modes taking into account the frictional effects

Enhanced propagation under OOP load pattern does not appear to be justified within a "LEFM description": in fact, as opposed to a simple shear, the superimposition of compression on an alternating shear leads to an increase in friction with a reduction in crack driving force [1, 9, 10] respect to simple shear. However the experimentally observed opening between the crack lips can significantly reduce the friction dissipation during the OOP tests. Since a simple model is not able to describe this complex material damage mechanism, the authors had employed a globally elastic micro-mechanical

model, capable of estimating the effective crack driving force ΔK_{III} by considering crack surface interaction under shear propagation [7]. The contacting peaks and valleys of the microscopically rough crack surfaces interact through a combination of sliding and sticking over some extent of the edge crack, thereby causing the smearing of the roughness asperities. The fracture surfaces interaction can significantly affect the loading cycle experienced by the material at the crack tip, since among the mating asperities on the crack faces normal contact stresses σ_c may arise, resulting in frictional shear stresses τ_f, acting in opposition to the applied shear stresses and proportional to the contact stress through the friction coefficient μ. Consequently the mode mixity of the stress intensity factors may be very different from that evaluated on the basis of the external loading.
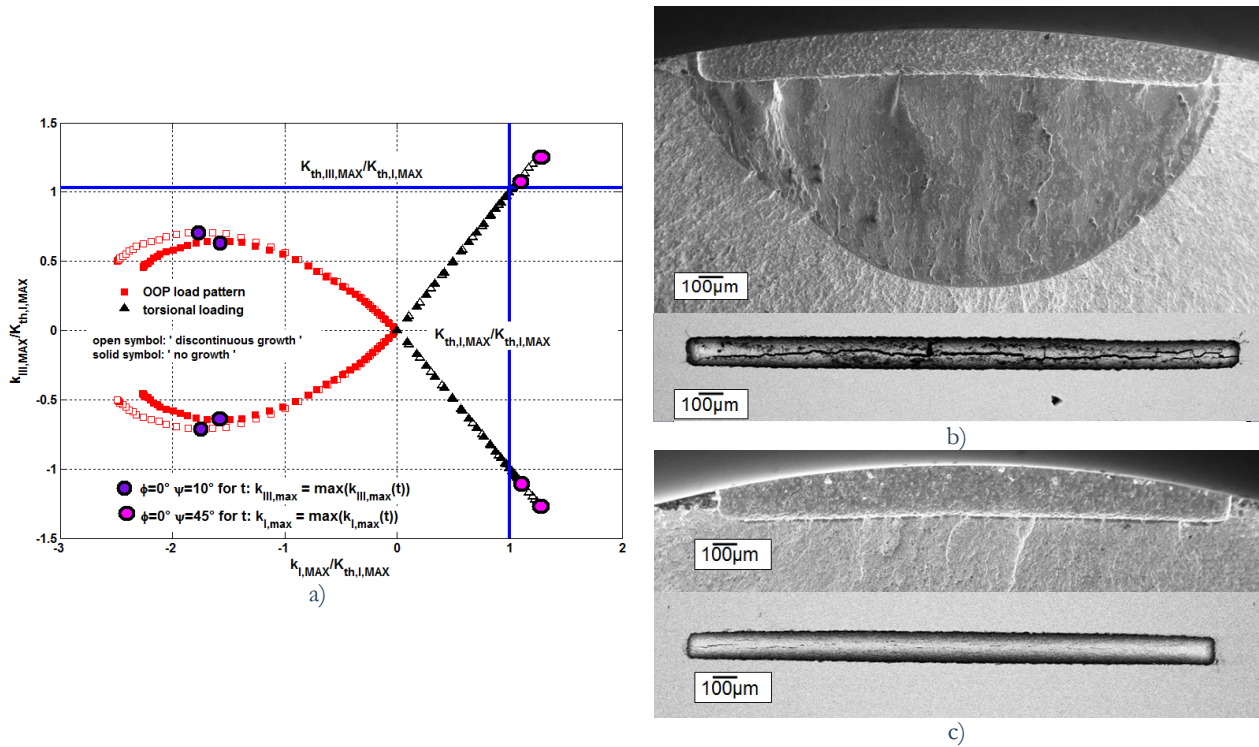
Figure 6: a) Competition between mode I and mode III crack branch stress intensity factors at the bottom of the defect (micro-notch size $\sqrt{area}$ = 630μm); b) top view and 90° tilted view of MOP load pattern corresponding to mode III 'discontinuous growth'; c) top view and 90° tilted view of OOP load pattern corresponding to mode III 'no growth' evidence.

The model used to estimate crack friction effects under OOP and torsion tests is based on assuming a 2D crack of depth a at the free surface of an elastic-plastic half space. The presence of three-dimensional effects can be neglected for the narrow defects since it has been shown that for $a/H > 1.2$ the K_{III} at the tip of a straight crack ahead of the notch rapidly approaches ($0.95 < K_{III,3D}/K_{III,2D} < 1$) the 2D solution for edge cracks (see Fig. 7a). The effective stress intensity factor at the tip of the crack is:

$$\Delta K_{III,eff} = \Delta K_{app} - 2K_f \tag{3}$$

where K_f is the 'frictional stress intensity factor' (the mode III stress intensity dissipated by friction) and factor 2 accounts for the frictional resistance at the maximum and minimum value of applied τ.
Moreover the frictional stress intensity factor K_f can be analytically calculated using the fracture mechanical weight function for the geometry configuration of an edge crack, Eq. (4):

$$K_f = \sqrt{\frac{a}{\pi}} \int_0^a \frac{\tau_f(x)}{\sqrt{a^2 - x^2}} dx \tag{4}$$

where

$$\tau_f(x) = \mu \sigma_c(x) \tag{5}$$

The extent of crack surface interaction and the possible contact pressure distribution can be obtained by respectively considering the crack opening (mode I) and sliding (mode III) displacements respectively. Once the shear displacements are greater than half the wavelength of the roughness, asperities are overcome and the resulting contact stresses distribution can be evaluated considering the crack opening displacement, at the end of the interaction zone, equal to the average height of the roughness (Figs. 7b-c). Details of the model could be found in [7].
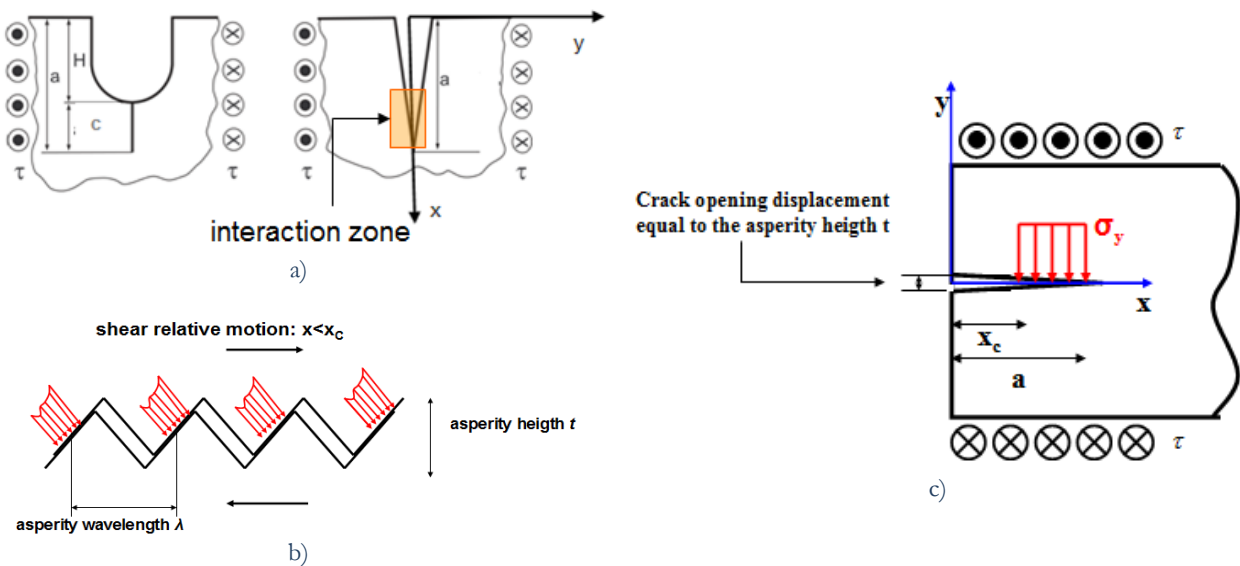
Figure 7: 2D partial-slip model: a) schematic of the 2D simplification of the shallow notch+crack under mode III; b) interlocking zone; c) pressure distribution.

Considering the effect of crack face friction the authors had found that the effective cyclic mode III threshold $\Delta K_{th,III,eff}$ under pure shear is smaller than the nominal threshold mode I threshold $\Delta K_{th,I}$ [7] thereby supporting the experimental evidence of mode III coplanar stable propagation in multiaxial OOP load pattern tests where the $\Delta K_{III,app}/\Delta K_{th,I}$ ratio is less than one. Moreover the application of the frictional analytical model had shown that typical crack opening values caused by the OOP load pattern prevent contact of the crack faces during the RCF load cycles, meaning that there is no friction of the crack faces and the $\Delta K_{th,III,OOP}$ measured corresponds to $\Delta K_{th,III,eff}$ [7]. In order to correctly estimate the contact stresses on the crack of Fig. 4 ($c = 520$ µm), the crack profile was accurately reconstructed by image processing (Fig. 8a) and the normal stresses $\sigma_c(x)$ were calculated by means of an analytical model based on the Newman crack closure model [11] suitably modified. This model is based on the superimposition of two elastic problems on the experimentally observed physical crack: a crack in a infinite plate subjected to both a remote compressive loading σ_∞ and a partial normal stress on its faces. The crack edges have been divided into n discrete bar elements and the length of an element along the crack profile, L_j, is proposed to be the experimentally observed crack opening. When the element length is smaller than the current crack-surface displacement due to the remote compressive loading, V_j, the element goes in contact and a normal stresses arises in order to make $V_j - L_j = 0$ (Fig. 8a).
It can be shown, see Fig. 8b, that if the maximum value of the effective mode III threshold $K_{th,III,MAX,eff}$ is used, it is finally possible to explain why the crack starts to propagate under mode III.

CONCLUSIONS

The results of an extensive new experimental campaign, previously developed by the authors on mode III coplanar crack propagation under pure shear and RCF loading conditions, were presented by pointing out the differences in the fracture mode of failures. The observation of the fracture surfaces confirm that:

- in torsional experiments at $\Delta K_{III} > 1$ there is the onset of coplanar shear growth with a discontinuous growth, which becomes stable for $\Delta KIII/\Delta K_{th,I} > 1$;

- in torsional experiments, where the values of ΔK_{III} at which there is the onset of co-planar propagation, even with a discontinuous growth, failures always occurred on planes tilted at 45°;

- in OOP load pattern (axial force always in compression) experiments, where $\Delta K_{th,III,OOP}$ is much lower than the threshold condition determined in pure torsion, the main failure mechanism is a shear type and the fracture morphology is perfectly planar: Mode I failure is prevented by the absence of positive K_I during the loading path.

The competition between mode I and mode III failure modes was analysed by calculating the stress intensity factors for a branch crack onto tilted planes during a loading cycle. The experimental fracture behaviour was confirmed by theoretical predictions when the partial slip model, previously employed by the authors, is used to analyze the load patterns in term of branch stress intensity factors.
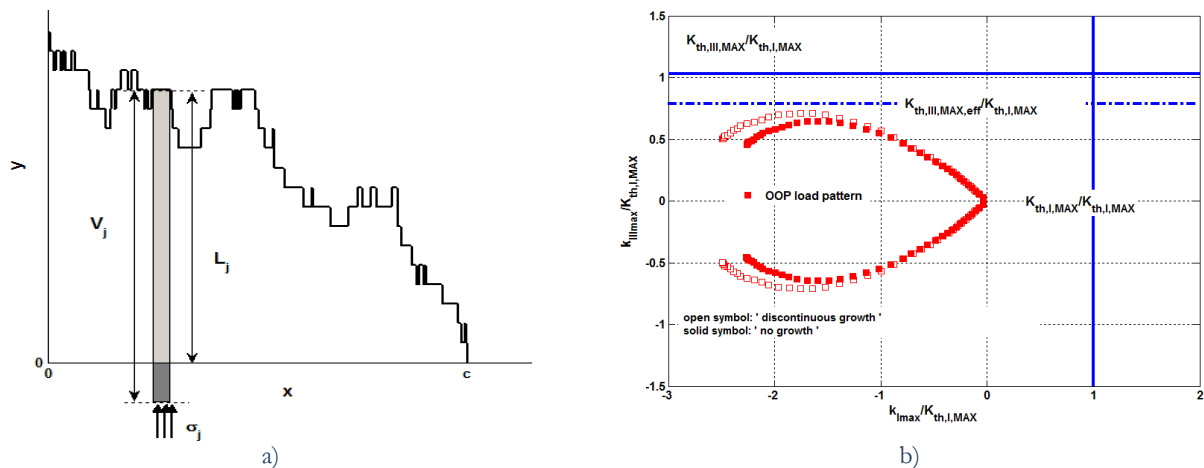
Figure 8: a) dicretized exmperimental OOP crack profile for the estimation of the contact pressure distribution by means of the Newman crack closure model; b) application of the frictional model to OOP load patterns tests: competition between tensile and shear failure modes (micro-notch size $\sqrt{area} = 630\mu m$).

REFERENCES

[1] Y. Murakami, Y. Fukushima, K. Toyama, S. Matsuoka, Engineering Fracture Mechanics, 75 (2008) 306.
[2] J. Pokluda, K. Slamecka, P. Sandera, Eng. Fract. Mech., 77 (2010) 1763.
[3] E.K. Tschegg, Material Science and Engineering, 54 (1982) 127.
[4] H. Nayeb-Hashemi, F. A. Mcclintock, R. O. Ritchie, International Journal of Fracture, 23 (1983) 163.
[5] S. Beretta, S. Foletti, K. Valiullin, Eng. Fract. Mech., 77 (2010) 1835.
[6] S. Beretta, S. Foletti, K. Valiullin, International Journal of Fatigue, 33 (2011) 287.
[7] M. G. Tarantino, S. Beretta, S. Foletti, J. Lai, A comparison of Mode III threshold under simple shear and RCF conditions. Engineering Fracture Mechanics (2011, in press).
[8] H. A. Richard, M. Fulland, Fat. Fract. Engng Mater. Struct., 28 (2005) 3.
[9] C. Pinna, V. Doquet, Fatigue Fract. Engng. Mater. Struct.; 22 (1999) 173.
[10] S. Melin, International Journal of Fatigue, 20 (1986) 103.
[11] J.C. Newmann, Jr, ASTM STP 748 (1981) 53.